Synergistic effects of previous winter NAO and ENSO on the spring dust activities in North China

Falei Xu[1], Shuang Wang[1], Yan Li[2], and Juan Feng[1]

[1]State Key Laboratory of Remote Sensing Science, Faculty of Geographical Science, Beijing Normal University, Beijing, China

[2]Key Laboratory for Semi-Arid Climate Change of the Ministry of Education, College of Atmospheric Sciences, Lanzhou University, Lanzhou, China

Correspondence: Juan Feng (fengjuan@bnu.edu.cn)

Abstract

Dust significantly influences global weather and climate by impacting the Earth's radiative balance. Based on the reanalysis datasets, this study explores how the North Atlantic Oscillation (NAO) and El Niño-Southern Oscillation (ENSO) during the preceding winter impact the following spring dust activities in North China. It is found that both the NAO and ENSO significantly affect dust activities in North China, especially during their negative phases. When both of them are in the negative phases, their combined impact on dust activities exceeding that of either factor individually. The previous winter NAO notably affects the sea surface temperatures (SST) in the North Atlantic, associated with an anomalous SST tripole pattern. These SST anomalies persist into the following spring due to their inherent persistence, inducing anomalous atmospheric teleconnection wave-train that influence dust activities in North China. ENSO, on the one hand, directly impacts dust activities in North China by modulating the circulation in the Western North Pacific. Moreover, ENSO enhances the NAO's effect on the North Atlantic SST, explaining their synergistic effects on dust activities in North China. This study elucidates the combined roles of NAO and ENSO in influencing dust activities in North China, providing one season ahead signals for predicting spring dust activities in North China.

1. Introduction

Dust, one of the most significant natural aerosols in the atmosphere, is of great importance to the global radiative balance with its light-absorbing properties, exerting a crucial role in climate change (Lou et al., 2017; Kok et al., 2023). Additionally, dust impacts not only its source regions but also extends its influence across oceans through teleconnections driven by atmospheric circulation. This transboundary transport affects ocean-atmosphere interactions and profoundly impacts the Earth's climate system (Huang et al., 2015). Dust activities, resulting from regional dust surges, pose formidable threats to socio-economic development, natural ecosystems, as well as human health and safety (Zhao et al., 2020; Li et al., 2023). The Gobi Desert in East Asia, particularly the Mongolian Plateau and Northern China, is a major source of dust (Chen et al., 2023), contributing approximately 70% of Asia's total dust emissions (Zhang et al., 2003). Given that China is profoundly impacted by dust activities (Fan et al., 2018), exploring the variations in dust activities over China is of great scientific and practical significance.

Besides the dust source regions over China (mainly Xinjiang and Inner Mongolia), dust content over North China also exhibits high values and strong interannual variability (Liu et al., 2004; Ji and Fan, 2019). Additionally, as a crucial center of politics, economy, and population, it is meaningful to investigate the variations of dust activities over North China (30-40°N, 105-120°E) and explore the relevant physical mechanisms. Previous studies have shown that the frequency of dust events in China exhibits strong variations, with high frequency from the 1950s to 1970s, low frequency from the 1980s to 1990s, and a notable increase after 2000 (Zhu et al., 2008; Ji and Fan, 2019). On interdecadal time scales, climate oscillations such as the Atlantic Multidecadal Oscillation (AMO), Pacific Decadal Oscillation (PDO), and Antarctic Oscillation (AAO) can influence dust activities by affecting the climatic background. For instance, the positive phase of PDO reduces dust activities by influencing the mid-latitude westerly regime, leading to weaker dust activities (uplift and deposition) in the Asian region (Gong et al., 2006). The AMO affects the global aridification process by altering the thermal properties between land and sea (Huang et al., 2017). Additionally, the AAO may substantially regulate dust activities in China by influencing the interaction of meridional circulations between the Northern and Southern Hemispheres (Ji and Fan, 2019).

On the interannual scale, a weaker East Asian Winter Monsoon is associated with anomalous circulation over the Gobi and Taklamakan deserts, facilitating the transport of dust, consequently increasing dust content in China (Lou et al., 2016). The variations of the sea ice coverage in the

Barents Sea significantly influence the intensity and frequency of dust activities in China by affecting cyclone generation and thermal instability in North China (Fan et al., 2018). The North Atlantic Oscillation (NAO) substantially impacts spring dust activities in North China by modulating the zonal wave-train from the Atlantic to the Pacific at mid-latitudes in the Northern Hemisphere, and the sea level pressure (SLP) gradient in the Tarim Basin in China (Zhao et al., 2013). On the synoptic scale, the NAO influences the emergence and evolution of dust activities in North China by impacting transient wave flux transport and atmospheric circulation (Li et al., 2023). Beyond extratropical signals, tropical variabilities, such as El Niño–Southern Oscillation (ENSO), also significantly modulate dust activities by regulating large-scale circulation, precipitation, and temperature variations over East Asia (Yang et al., 2022), Saudi Arabia (Yu et al., 2015), and North America (Achakulwisut et al., 2017).

From the aforementioned studies on dust activities in China, it is evident that the NAO and ENSO are two important factors, with a focus on their individual effects on the dust activities in China. However, as significant climate variabilities in the extratropical and tropical regions, respectively, the NAO and ENSO often co-occur and have complex interactions (López-Parages et al., 2015). It is found that ENSO can influence the climate near the North Atlantic through atmospheric forcing of the Pacific-North America teleconnection (Wallace and Gutzler, 1981). During the early winter of El Niño events, strong convective anomalies in the tropical Indian Ocean-Western Pacific (Abid et al., 2021) and the Gulf of Mexico-Caribbean Sea (Ayarzagüena et al., 2018) can trigger Rossby wave-train reaching the North Atlantic, leading to positive NAO signals. Furthermore, the stratosphere, serving as an energy transmission channel, may also be an important pathway for ENSO to influence the NAO (Jiménez-Esteve and Domeisen, 2018). Moreover, observations and numerical simulations have demonstrated that the NAO can induce a Gill-Matsuno pattern in the tropical region, strengthening the connection between the East Asian Summer Monsoon and ENSO (Wu et al., 2012). When the NAO is in its positive phase, intensified northeasterlies over tropical North Atlantic are observed, increasing low-level moisture content and precipitation in the tropical North Atlantic, which in turn enhances ENSO's impact (Ding et al., 2023). These studies emphasize the connections and interactions between NAO and ENSO, underscoring the necessity of considering their synergistic effects on the dust activities in North China.

The synergistic effect refers to the phenomenon where the combined impacts of two or more factors are significantly greater than their individual roles (Li et al., 2019). It has been found that there are synergistic effects in the impact of NAO and ENSO on the weather and climate in China.

The NAO can facilitate the development of the subpolar teleconnection across northern Eurasia downstream, leading to anomalies in the high-pressure systems over the Ural Mountains and the Sea of Okhotsk, which in turn affect the East Asian Summer Monsoon (Wang et al., 2000). Meanwhile, ENSO exerts significant impact on the convective activities in the central Pacific and induces alterations in the equatorial circulation via the Pacific-East Asia teleconnection, further affecting the atmospheric circulation and sea surface temperature (SST) in the Western North Pacific (WNP), ultimately influencing the intensity of the East Asian Summer Monsoon (Wang et al., 2000). Therefore, the synergistic effects of NAO and ENSO can result in pronounced impacts on the East Asian Summer Monsoon. During El Niño events, SST in the central and eastern equatorial Pacific rises, enhancing convective activity near the equator, which brings more moisture to Northern China and increases the likelihood of precipitation. Simultaneously, the positive phase of NAO can alter atmospheric pressure in the North Atlantic, influencing atmospheric circulation over the Eurasian continent. The influences of NAO and ENSO synergistically regulate the distribution of precipitation in Northern China (Guo et al., 2012).

The synergistic effects of NAO and ENSO significantly influence the climate in China, but their synergistic effects on the spring dust activities over North China and the mechanisms involved remain unclear. This study will investigate these effects on dust activities over North China, providing a scientific foundation for predicting dust activities in China. The structure of this paper is as follows: Section 2 outlines the datasets and methods employed in this study. Section 3 presents the analysis and findings. Section 4 contains the conclusions and discussions.

2. Datasets and methods

2.1 Datasets

The dust dataset for the Modern-Era Retrospective Analysis for Research and Applications Version 2 (MERRA-2) was obtained from NASA's Global Modeling and Assimilation Office (GMAO), incorporating assimilated observations from both satellites and ground stations (Gelaro et al., 2017). In this study, the Dust Column Mass Density of the MERRA-2 tavg1_2d_aer_Nx product was utilized to represent the dust content with a $0.5° \times 0.625°$ resolution from 1980-2022. Previous studies have demonstrated the applicability of MERRA-2 reanalysis data for representing the spatiotemporal distribution characteristics of dust content in China (Kang et al., 2016; Wang et al., 2021). It is reported that the results based on MERRA-2 are similar to those obtained from MODIS, OMPS, CALIPSO, and Himawari-8 datasets (Kang et al., 2016; Wang et al., 2021).

Additionally, we further employ the datasets from the China National Meteorological Centre from 1980-2018, which include observations of floating dust, blowing dust, and dust storms, to validate the reliability of MERRA-2 reanalysis dataset. The frequency of dust activities recorded at these stations has been converted into a Dust Index (DI) (Wang et al., 2008; Equations 1), effectively representing the dust content.

$$\mathrm{DI} = 9 \times \mathrm{DS} + 3 \times \mathrm{BD} + 1 \times \mathrm{FD} \quad (1)$$

Where DS, BD, and FD represent the frequency of dust storms, blowing dust, and floating dust, respectively. Additionally, DI denotes the dust content at each station. It is worth noting that the value of 1 represents the normalized mass weight of dust content for each FD, while 3 and 9 represent the relative mass weight of dust content for BD and DS, respectively (Wang et al., 2008). Therefore, DI is an index used to indicate the dust content which does not have unit. In order to better compare the DI with the reanalysis, we first interpolate the site data into grid points by Cressman (1959), and then obtain the gridded DI. We found that the distribution of DI and MERRA-2 dust content during the four seasons all show similar spatial characteristics (Figure 1). The above results indicate that the MERRA-2 reanalysis data can capture the spatiotemporal characteristics of dust content in China, which is applicable to understand the variations in dust content in China.

Additionally, the SST dataset was derived from the Hadley Centre of the UK Met Office on a 1°×1° grid (Rayner et al., 2003). The atmospheric reanalysis datasets employed herein were provided from the Fifth Generation Reanalysis Version 5 (ERA-5) of the European Centre for Medium-Range Weather Forecasts (ECMWF) with a resolution of 0.25°×0.25° on 37 vertical levels (Hersbach et al., 2020). The period of SST and atmospheric reanalysis datasets was from 1979-2022. The winter is defined as the average of December-February (December-January-February, DJF), with the winter 1979 (2021) corresponding to the average of December in 1979 (2021), January and February in 1980 (2022). The spring seasonal mean is the average of March, April, and May. Thus, the previous winter is from 1979 to 2021, and the following spring is from 1980 to 2022. To focus the investigation into the interannual variability, the linear trends of all variables were removed.

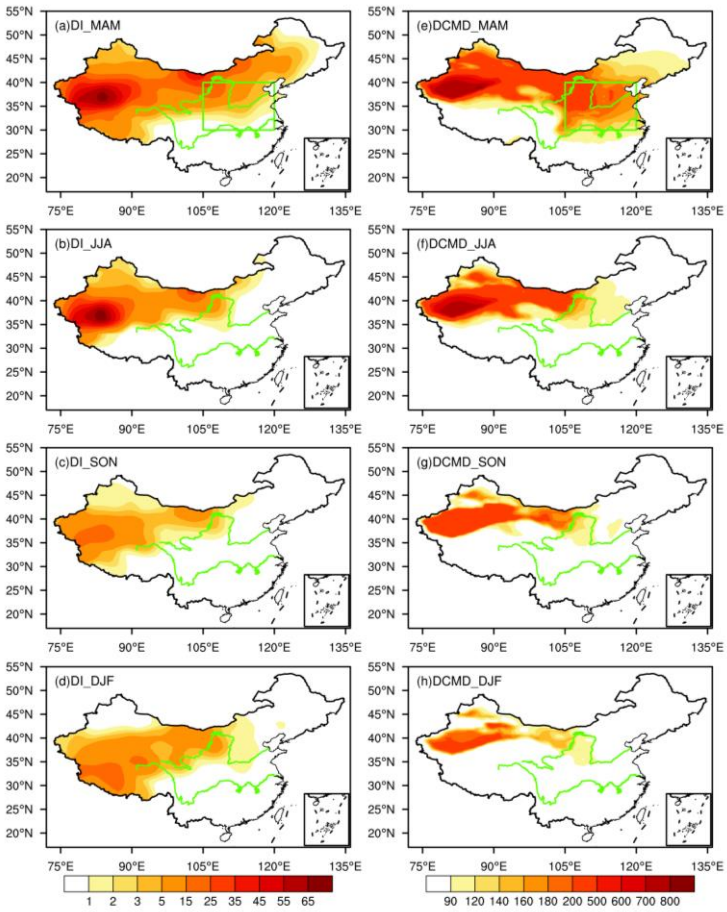

Figure 1. (a-d) Spatial distribution of seasonal mean DI based on station data, (e-h) as in (a-d), but for dust column mass density based on MERRA-2 (units: $mg \cdot m^{-2}$). The green box in (a) and (e) represents North China. The green lines represent the Yellow River (northern one) and the Yangtze River (southern one), respectively.

2.2 Methods

The NAO index (NAOI) used is following Li and Wang (2003), quantified by the difference in the normalized monthly SLP regionally zonal averaged over the North Atlantic within 80°W-30°E between 35°N and 65°N. This definition effectively captures the large-scale circulation characteristics associated with NAO, essentially measuring the intensity of zonal winds spanning the entire North Atlantic. We also employed the NAOI from Hurrell (1995) and Jones (1997) to validate the NAOI by Li and Wang (2003). A good agreement with correlation coefficients of 0.96 and 0.94 between these two indices and the NAOI defined by Li and Wang (2003). Furthermore, ENSO is characterized by Niño3.4 index with SST anomalies averaged over 5°S-5°N, 170°W-120°W (Trenberth, 1997).

In this study, the seasonal standardized values exceeding 0.5 standard deviation identified as anomalous years. The correlation analysis is used to examine the relationship between NAO/ENSO

and dust content over North China, while composite analysis investigates the synergistic effects of these climatic variabilities on dust activities over North China. The statistical significance of the correlation, regression, and composite values is assessed using a two-sided Student's *t*-test. Unless otherwise noted, all reported statistically significant levels are at the 0.1 level.

The memory effect of SST can be elucidated by the SST persistence component (SST_p), as delineated in equation (2) (Pan, 2005).

$$SST_p = SST(t) * \frac{Cov[SST(t), SST(t+1)]}{Var[SST(t)]} \tag{2}$$

SST_p represents the memory effect of the previous SST (t; previous winter) on the following SST ($t+1$; spring), where $SST(t)$ and $SST(t+1)$ denote the previous winter SST and spring SST, respectively. $Cov[SST(t), SST(t+1)]$ denotes the covariance between the previous winter SST and spring SST, while $Var[SST(t)]$ signifies the variance of the previous winter SST. Consequently, the $Cov[SST(t), SST(t+1)]/Var[SST(t)]$ represents the connection between the SST variations in previous winter and spring. A greater value of SST_p indicates the variation of $SST(t+1)$ is more closely attached with the variation of $SST(t)$.

The T-N wave activity flux (WAF), formulated by Takaya and Nakamura (2001), represents a three-dimensional wave action flux that describes the energy dispersion characteristics of stationary Rossby waves, thereby reflecting the direction of Rossby wave energy dispersion. The WAF is suitable for application in mid-high latitude regions where the background circulation deviates from uniform zonality, as obviates the need for the assumption that the basic flow field must be a zonally averaged basic flow and can accommodate zonally non-uniform wind fields. The convergence and divergence characteristics of WAF reveal the source and dissipation areas of wave energy, with the transmission direction indicating the direction of energy transport. The three-dimensional formulation of WAF is as follows:

$$W = \frac{pcos\varphi}{2|\boldsymbol{U}|} \cdot \begin{pmatrix} \frac{U}{a^2 cos^2\varphi}\left[\left(\frac{\partial\psi'}{\partial\lambda}\right)^2 - \psi'\frac{\partial^2\psi'}{\partial\lambda^2}\right] + \frac{V}{a^2 cos\varphi}\left[\frac{\partial\psi'}{\partial\lambda}\frac{\partial\psi'}{\partial\varphi} - \psi'\frac{\partial^2\psi'}{\partial\lambda\partial\varphi}\right] \\ \frac{U}{a^2 cos\varphi}\left[\frac{\partial\psi'}{\partial\lambda}\frac{\partial\psi'}{\partial\varphi} - \psi'\frac{\partial^2\psi'}{\partial\lambda\partial\varphi}\right] + \frac{V}{a^2}\left[\left(\frac{\partial\psi'}{\partial\varphi}\right)^2 - \psi'\frac{\partial^2\psi'}{\partial\varphi^2}\right] \\ \frac{f_0^2}{N^2}\left\{\frac{U}{acos\varphi}\left[\frac{\partial\psi'}{\partial\lambda}\frac{\partial\psi'}{\partial z} - \psi'\frac{\partial^2\psi'}{\partial\lambda\partial z}\right] + \frac{V}{a}\left[\frac{\partial\psi'}{\partial\varphi}\frac{\partial\psi'}{\partial z} - \psi'\frac{\partial^2\psi'}{\partial\varphi\partial z}\right]\right\} \end{pmatrix} \tag{3}$$

In the expression, p, φ, λ, f_0, and a represent the atmospheric pressure, latitude, longitude, Coriolis parameter, and Earth's radius, respectively. $\psi' = \Phi'/f_0$ (where Φ represents the geopotential height) denotes the disturbance of the quasi-geostrophic stream function relative to the climatology. N is buoyancy frequency, $z = -Hln(p)$ with H being a constant scale height (H=8

km). The basic flow field $\boldsymbol{U} = (U, V, Z)$ (where Z represents the selected level) denotes the climatic field, where U and V indicate the zonal and meridional velocities, respectively.

3. Results

3.1 Impacts of NAO and ENSO on the spring dust in North China

The NAO shows the strongest variability during the winter months, with the maximum standard deviation in February (Figure 2a). Similarly, ENSO shows larger variation during winter (Figure 2b). Previous studies have found that preceding NAO and ENSO significantly impact the subsequent climate over North China, particularly the cross-seasonal impacts (Zheng et al., 2016a; Feng et al., 2019). We have examined the roles of the previous autumn, winter and simultaneous spring NAO and ENSO on the spring dust over North China. It is found that the most significant influences on spring dust occur when NAO and ENSO lead by one season (Figures 2c-h). Therefore, the impacts of the previous winter NAO and ENSO on spring dust over North China are discussed in the study.

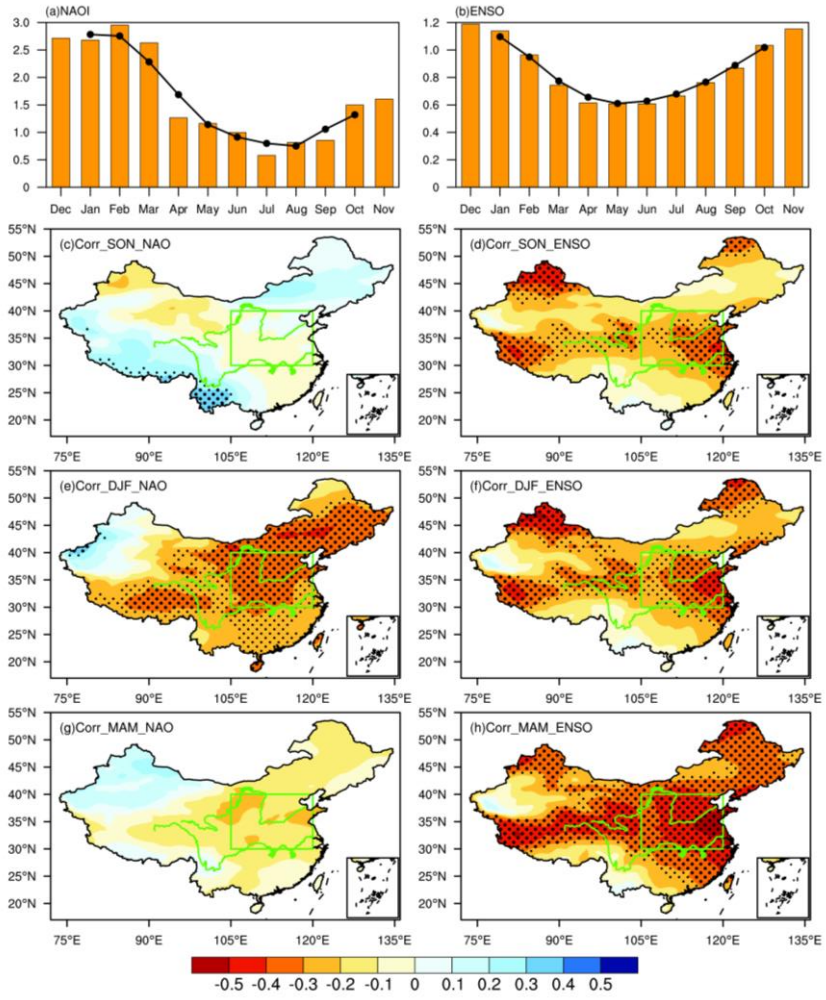

Figure 2. The monthly standard deviation of (a) NAOI and (b) Niño3.4 index, respectively. Black line represents three-month running average of standard deviation. (c) Spatial distribution of correlation coefficients between the previous autumn NAOI and spring dust content . (d) As in (c), but with Niño3.4 index. (e-f) and (g-h), as in (c-d), but for the correlations with previous winter and simultaneous spring NAOI and Niño3.4 index, respectively. The green box represents North China. Thick and fine stippled areas are statistically significant at the 0.05 and 0.1 level, respectively. The green lines in (c-h) represent the Yellow River (northern one) and the Yangtze River (southern one), respectively.

The results indicate that lower (higher) dust content is expected when the NAO and ENSO are in the positive (negative) phases (Figures 2e-f). Meanwhile, the NAOI/Niño3.4 index is significantly correlated with the area-averaged spring dust content over North China (SDI), with correlation coefficients of -0.36/-0.35 statistically significant at the 0.1 level. Considering the significant relationship between the NAO and ENSO (López-Parages et al., 2015; Zhang et al., 2015), to detect their independent effects on the dust content, the partial correlation between NAO (ENSO) and dust content after removing the influence of the ENSO (NAO) is provided (Figures 3a-b). The results indicate that the significant correlation regions between dust content and either NAO or ENSO show little change after removing the influence of the other. These findings suggest a stable and significant connection between the previous winter NAO/ENSO and SDI.

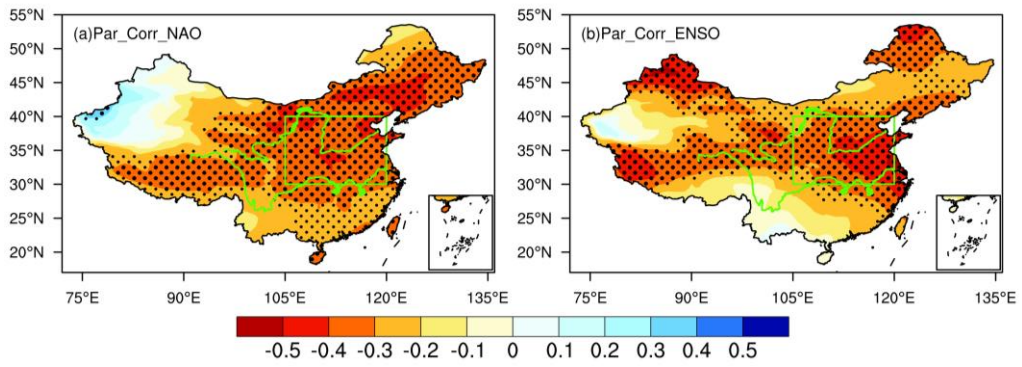

Figure 3. (a) Spatial distribution of partial correlation coefficients between the previous winter NAOI and spring dust content after removing the effect of ENSO. (b) As in (a), but for correlation between Niño3.4 index and dust content after removing the effect of NAO. The green box represents North China. Thick and fine stippled areas are statistically significant at the 0.05 and 0.1 level, respectively. The green lines represent the Yellow River (northern one) and the Yangtze River (southern one), respectively.

Previous studies have indicated that the development rate, intensity variations, and spatial structure of the NAO exhibit distinct asymmetries between different phases (Feldstein, 2003; Jia et al., 2007). And the influence of NAO on the East Asian Winter Monsoon is more pronounced during its negative phase (Sung et al., 2010). In addition, it is shown that El Niño and La Niña, as the positive and negative phases of ENSO, are not simply mirror images of each other. The SST

anomalies in the tropical Pacific associated with ENSO exhibit significant asymmetries in meridional range (Zhang et al., 2009), amplitude (Su et al., 2010), zonal propagation (McPhaden and Zhang, 2009), and impacts (Feng and Li, 2011; Feng et al., 2020) under El Niño and La Niña conditions. To further explore these asymmetries, we analyzed the connection between NAO/ENSO and SDI during different phases. The results indicate that the relationship between NAO/ENSO and SDI also exhibits significant asymmetry, i.e., with weaker (stronger) correlations during their positive (negative) phases (Figure 4). Based on the scatter distribution of SDI under different phases of NAO and ENSO, it is noted that the correlation coefficients between NAOI and SDI during the positive and negative phases of NAO are -0.05 (statistically insignificant) and -0.46 (statistically significant), indicating that the significant influence of NAO on the SDI mainly occurs during its negative phase (Figure 5a). Similarly, the correlation coefficients between ENSO and SDI also shows that the influence of ENSO is more pronounced during its negative phase, with the correlation coefficients for the positive and negative phases being -0.16 (statistically insignificant) and -0.36 (statistically significant), respectively (Figure 5b). These results demonstrate that the impacts of the previous winter NAO and ENSO on the SDI exhibit asymmetrical characteristics, with significant effects primarily manifested during their negative phases.

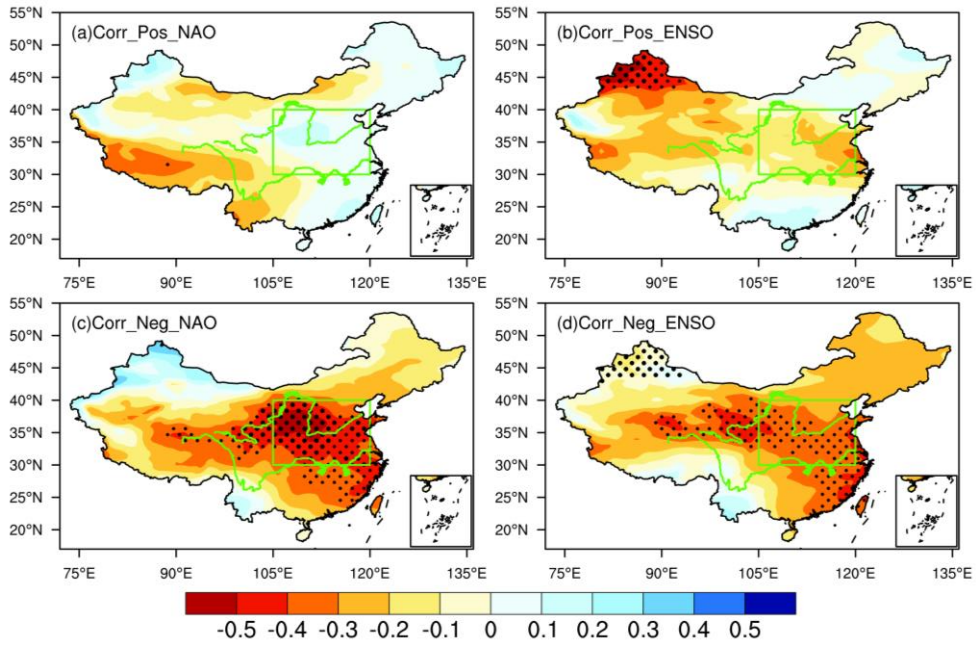

Figure 4. Spatial distribution of correlation coefficients between (a) positive and (c) negative NAO phases and dust content. (b) and (d) as in (a) and (b), respectively, but for the Niño3.4 index. The green box represents North China. Thick and fine stippled areas are statistically significant at the 0.05 and 0.1 level, respectively. The green lines represent the Yellow River (northern one) and the Yangtze River (southern one), respectively.

The synergistic effects of climate variabilities from mid-high latitudes and the tropics are pivotal mechanisms affecting the weather and climate in East Asia (Feng et al., 2019; Li et al., 2019). Correspondingly, we will examine whether the negative phases of the previous winter NAO and ENSO exert synergistic effects on the dust content over North China. As shown in Figure 5c, when the NAO is in its negative phase (Table 1; white bar in Figure 5c labeled NAO), the value of anomalous SDI is +16.21 mg·m^{-2} (statistically significant), whereas it is +8.32 mg·m^{-2} (statistically insignificant) for the case that negative NAO occurred alone (red bar in Figure 5c). Similarly, the value of anomalous SDI in the negative ENSO phase is greater than that when negative ENSO occurred alone (+19.40 mg·m^{-2} (statistically significant) vs. +14.88 mg·m^{-2} (statistically insignificant)). When both the NAO and ENSO are in their negative phases (Table 1), the value of anomalous SDI (+25.23 mg·m^{-2}; statistically significant) is much greater than the situation when one of them is in the negative phase (green bar in Figure 5c). This indicates that the negative phases of the previous winter NAO and ENSO demonstrate synergistic effects on the dust content over North China. Therefore, three categories, i.e., the NAO/ENSO is in its negative phase, and both the NAO and ENSO are in the negative phases (Table 1) are discussed in the context, to elucidate the relevant processes of the synergistic effects of NAO and ENSO on the dust content over North China.

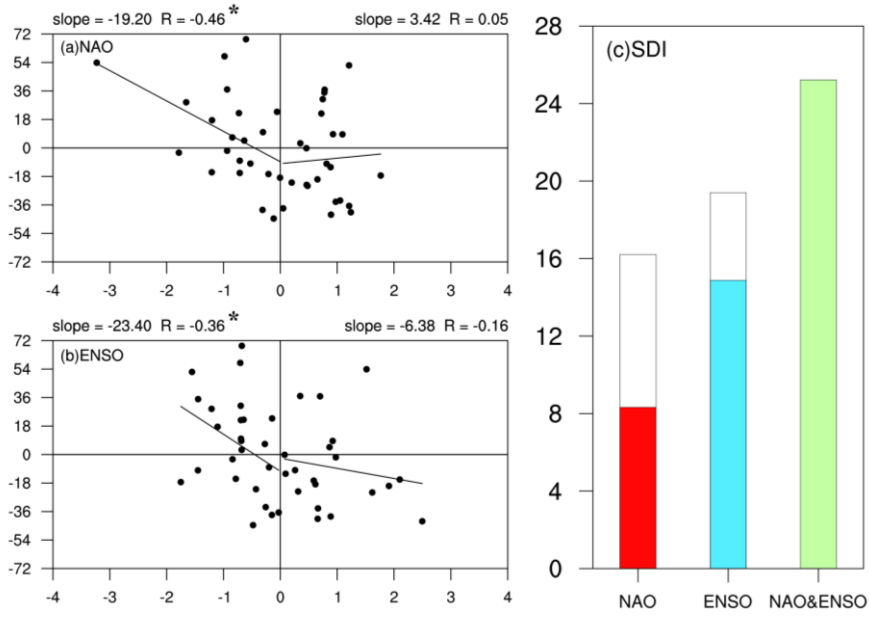

Figure 5. Scatterplots of the spring dust content in North China against previous winter (a) NAOI and (b) Niño3.4 index. Also shown are lines of best fit for positive and negative NAOI/Niño3.4 index values and correlation coefficients (R), slope (slope), * indicates statistically significant at the 0.1 level. (c) Spring dust content over North China during the negative NAO, negative ENSO phases, and concurrent negative phases of NAO and ENSO (unit: mg·m^{-2}). White bars represent negative phases of the NAO and ENSO, red and blue bars indicate solo negative NAO and ENSO years, and green bar is the negative NAO and ENSO co-occurring years.

Table 1. The events of NAO and ENSO classified by three categories

Scenarios	Years	Numbers
NAO^-	1980,1982,1985,1986,1987,1996,1998,2001, 2003,2004,2006,2010,2011,2013,2021	15
$ENSO^-$	1984,1985,1986,1989,1996,1999,2000,2001, 2006,2008,2009,2011,2012,2018,2021,2022	16
NAO^- &$ENSO^-$	1985,1986,1996,2001,2006,2011,2021	7

3.2 Impacts of NAO and ENSO on the environmental variables

To examine the anomalous characteristics associated with NAO and ENSO, the circulation anomalies in their negative phases, as well as in their co-occurring negative phases (Table 1) are analyzed. In the upper troposphere (200 hPa), zonal wind intensifies over northwest China and Mongolia during the negative NAO phase (Figure 6a), with significant positive anomalies centered over Mongolia. In the negative ENSO phase, intensified zonal winds over northwest China and Mongolia are observed in the upper level (Figure 6d). The intensification of upper-level zonal wind boosts the upper-level momentum, which is transferred downward to the mid-lower troposphere through vertical circulation (Wu et al., 2016; Li et al., 2023), causing windy weather in the dust source regions, facilitating dust lifting and transport activities, thereby promoting the occurrence of dust activities in the downstream North China. When both the NAO and ENSO are in their negative phases, the primary positive anomaly center appears over the northern part of North China, facilitating dust transport to North China. The result implies the synergistic effects of NAO and ENSO on the upper-level zonal wind, enhancing dust transport from source regions to North China, favoring for dust activities in North China (Figure 6g).

Subsequent analysis delved into the anomalous distribution of the circulation field in the mid and lower troposphere. In the negative NAO situation, a pronounced trough-ridge anomaly pattern emerges in the mid-latitude region, characterized by a trough in Siberia and a ridge in the Middle East (Figure 6b). This atmospheric configuration fosters a dominant meridional circulation in the mid-high latitude region, enhancing the southward transport of cold air from the north. This incursion of cold air strengthens surface wind speeds, promoting the uplift and transport of dust from source regions. In the negative ENSO situation, a similar trough-ridge pattern is observed in the mid-latitude, but with more pronounced circulation anomalies over the WNP. The region is predominantly under the influence of northeasterly winds on its western flank, manifesting cyclonic circulation anomalies (Figure 6e). This abnormal circulation hinders the northward transport of warm and moist air from the South China Sea and the Bay of Bengal, diminishing the likelihood of

interactions with cold air from the north, thus reducing the likelihood of formation of stationary fronts and precipitation. The decrease in precipitation weakens the wet deposition (Zheng et al., 2016b; Huang et al., 2021), favoring the occurrence of dust activities in North China. When both the NAO and ENSO are in their negative phases, the meridional circulation in the mid-latitude region is enhanced (Figure 6h). The southward shift of the trough-ridge pattern significantly increases wind speeds in the upstream dust source regions of North China, providing a substantial source of dust for North China. Additionally, the presence of cyclonic circulation anomalies over the WNP reduces the transport of warm and moist air from the south, which is unfavorable for precipitation. This reduction in precipitation suppresses the wet deposition , favoring the occurrence and intensification of dust activities in North China.

As for the SLP, significant positive anomalies appear in Eastern Europe and Russia during the negative NAO situation, indicating the Siberian High (SH) is intensified and extended southward to the dust source regions upstream of North China (Figure 6c). The intensification of the SH is typically accompanied with strong northerlies and dry conditions, which favor the transport of dust, thereby supplying abundant material sources for dust activities in North China. In the negative ENSO case, although the high-latitude region exhibits a weaker SH signal, significant circulation anomalies occur over the WNP. This cyclonic circulation anomalies inhibit the northward transport of warm and moist air from the south, leading to unfavorable precipitation conditions in North China (Figure 6f). When both the NAO and ENSO are in their negative phases, the intensify and extent of the SH are more pronounced compared to that when the NAO sole is in negative phase. Additionally, cyclonic circulation anomalies persist over the WNP, which are conducive to the occurrence of dust activities in North China (Figure 6i).

The results suggest that when both the NAO and ENSO are in their negative phases, synergistic effects emerge, rendering the atmospheric circulation anomalies in the troposphere more conducive to dust activities in North China. The synergistic effects likely result from the superposition and interaction of various atmospheric levels modulated by the NAO and ENSO, forming favorable circulation conditions for dust activities in North China.

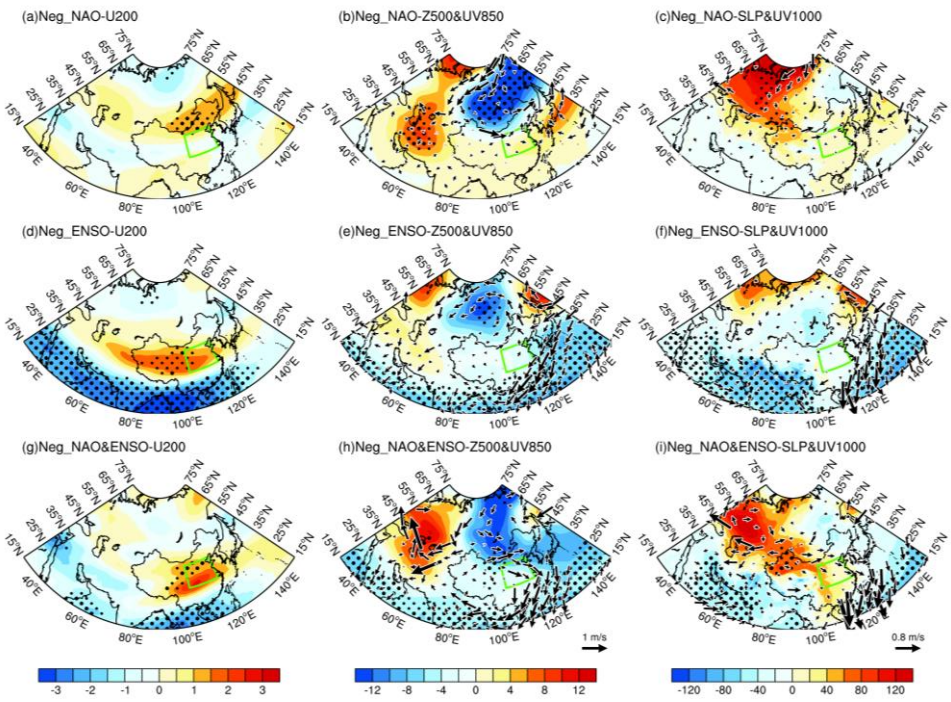

Figure 6. Upper, the composite anomalies of (a) 200 hPa zonal wind (shading, unit: $m \cdot s^{-1}$), (b) 500 hPa geopotential height (shading, unit: gpm) and 850 hPa wind field (arrows, unit: $m \cdot s^{-1}$), (c) sea-level pressure (shading, unit: Pa) and 1000 hPa wind field (arrows, unit: $m \cdot s^{-1}$) during the negative NAO phases. Middle-Lower, as in the upper, but during the negative ENSO phases and co-occurred negative phases of NAO and ENSO, respectively. The green box represents North China. Only wind anomalies statistically significant at the 0.1 level are shown. Thick and fine stippled areas are statistically significant at the 0.05 and 0.1 level, respectively.

Dust activities are not only impacted by large-scale circulation patterns, and also influenced by local surface conditions and meteorological processes. Surface properties and local meteorological factors play ignore roles in the initiation, development, and dissipation of dust activities (Liu et al., 2004; Huang et al., 2021). In particular, humidity and precipitation are decisive factors in determining the frequency and intensity of dust activities (Prospero et al., 1987; Kim and Choi, 2015). Low humidity leads to drier soil conditions in dust source regions, reducing soil particle cohesion and facilitating dust lifting and transport (Csavina et al., 2014). Similarly, less precipitation weakens wet deposition, resulting in higher dust content (Zheng et al., 2016b). Therefore, we further analyzed the potential impacts of the NAO and ENSO on humidity and precipitation. During the negative NAO phase, humidity and precipitation slightly decrease in northern northwest China, impacting dust lifting and transport in the dust source regions (Figures 7a-b). In the negative ENSO phase, the variations in humidity and precipitation are similar to that as in the negative NAO, but with greater amplitude (Figures 7c-d). When both the NAO and ENSO are in their negative phases, the humidity and precipitation anomalies in the dust source regions are more intense than those caused by the individual factors (Figure 7e-h). The NAO and ENSO modulate humidity and

precipitation by affecting atmospheric circulation anomalies, ultimately affecting dust activities in North China. During the negative NAO case, the diminished atmospheric pressure gradient in the mid-high latitude regions of the North Atlantic leads to the intensification and southward shift of the SH (Zhou et al., 2023), accompanied by strong wind, making the environment drier and conducive to dust lifting and transport in dust source regions. In the negative ENSO case, the upper atmosphere over the WNP is dominated by significant negative anomalies in geopotential height and northeasterly winds (Zhang et al., 2015), reducing moist air transport. When both the NAO and ENSO are in their negative phases, their regulation on the atmospheric circulation produces synergistic effects, further promoting the occurrence of dust activities in North China.

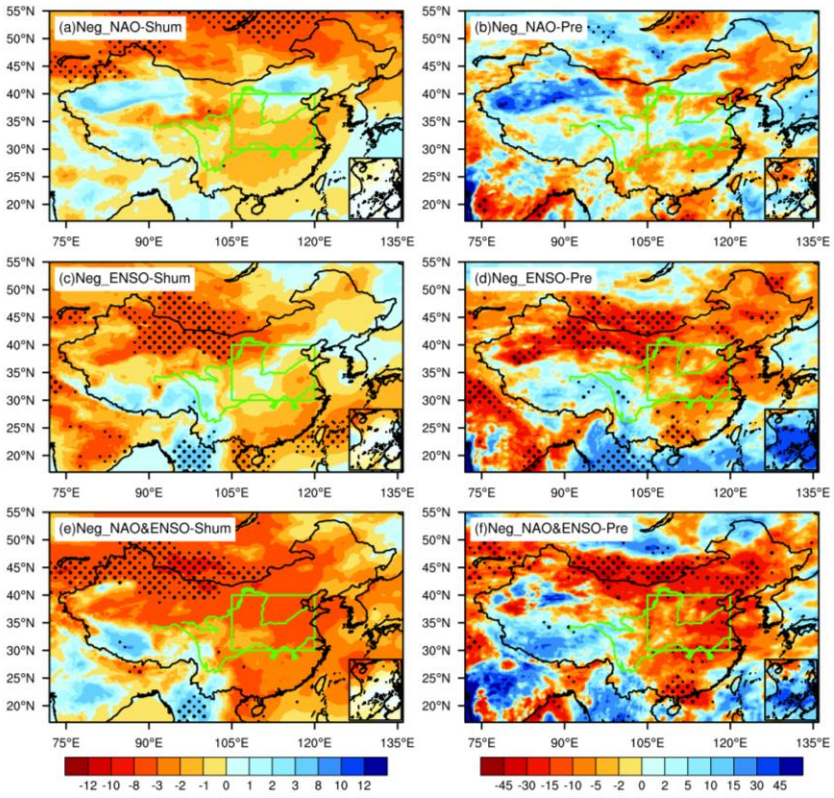

Figure 7. As in Figure 6, but for the composite percentage anomalies of (Left) special humidity and (Right) precipitation.

3.3 Physical Mechanisms of the NAO and ENSO on the dust activities

The above results demonstrate that the previous winter NAO and ENSO significantly impact spring dust activities in North China. Consequently, an examination of the underlying physical mechanisms is warranted. The previous ENSO signal can alter the atmospheric circulation over the WNP through the persistent impact of SST, affecting subsequent weather and climate in China (Kim and Kug, 2018; Jiang et al., 2019). Given the relatively short memory of NAO as an atmospheric

phenomenon, we will employ the theory of ocean-atmosphere coupling bridge to elucidate the involved processes. The tripole configuration of SST is the leading mode of SST variation in the North Atlantic, and its variabilities are closely associated with the NAO (Wu et al., 2009). This association allows the previous NAO signal to exert a long-term influence on subsequent weather and climate in China (e.g., Chen et al., 2020; Wu and Chen, 2020; Song et al., 2022). The variation of the SDI is linked with an anomalous tripole SST in the North Atlantic (Figure 8a), paralleling the SST anomalies associated with the negative phase of the NAO. Therefore, the North Atlantic tripole index (NATI) is defined to depict the characteristics of SST anomalies (Equations 4-7). The correlation analysis between the high and low years of SDI and SST reveals a pronounced difference, indicating an asymmetric correlation (Figures 8b-c). Specifically, the significant relationship between SDI and NATI only exists in the positive SDI years, with a significant correlation coefficient of -0.47, implying that the occurrence of NATI would associate with more dust activities over North China.

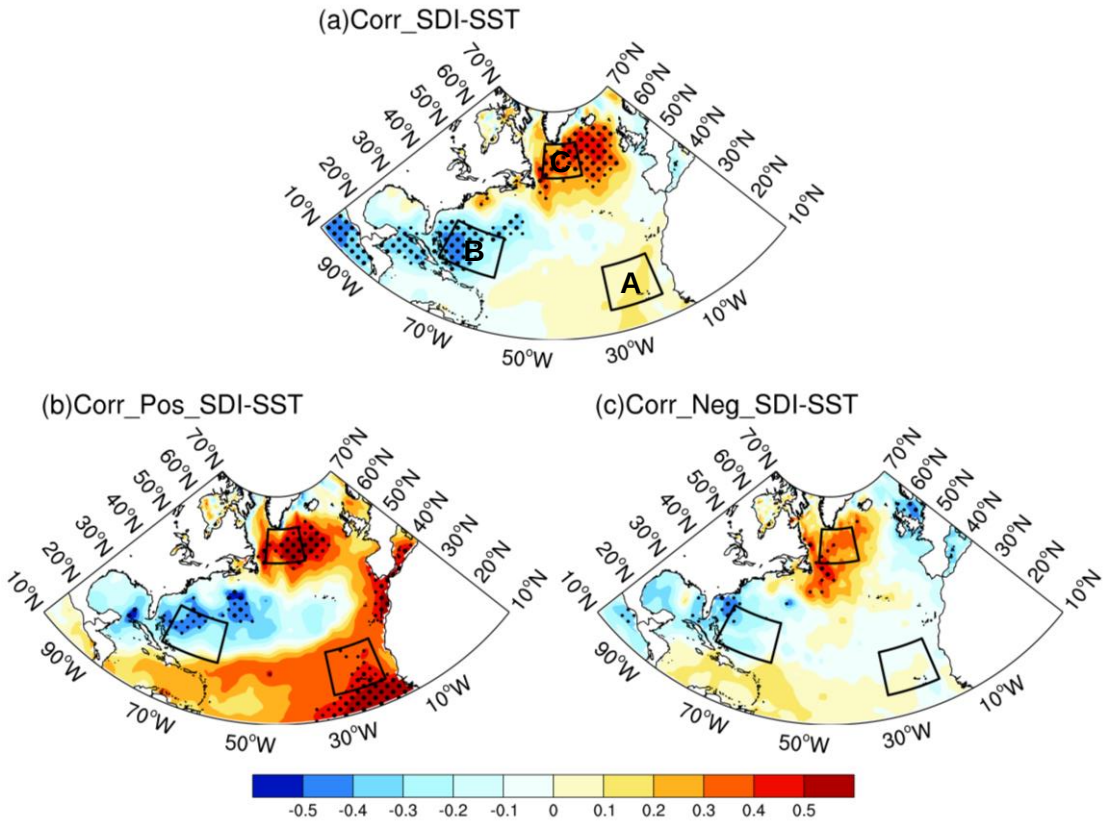

Figure 8. (a) Spatial distribution of the correlation coefficients between the SDI and simultaneous SST. (b)-(c) As in (a), but for the positive and negative phases of SDI. Thick and fine stippled areas are statistically significant at the 0.05 and 0.1 level, respectively. The black box represents NATI.

$$\mathrm{SST_A} = [15{-}25^{\circ}\mathrm{N}, 32{-}20^{\circ}\mathrm{W}] \quad (4)$$

$$\mathrm{SST_B} = [22{-}32^{\circ}\mathrm{N}, 75{-}60^{\circ}\mathrm{W}] \quad (5)$$

$$\mathrm{SST_C} = [50{-}60^{\circ}\mathrm{N}, 50{-}32^{\circ}\mathrm{W}] \quad (6)$$

$$\mathrm{NATI} = \mathrm{SST_B} - \frac{1}{2}(\mathrm{SST_A} + \mathrm{SST_C}) \quad (7)$$

Moreover, the relationship between the previous winter NAOI and spring NATI is only manifested during the negative phase of NAO, with a statistical significant correlation coefficient of 0.41 (figures not shown). This elucidates the reason why the significant impact of NAO on dust activities in North China only existed during its negative phase. The correlations between the previous winter NAO and North Atlantic SST reveal that NAO is linked with an anomalous tripole SST pattern during the NAO negative situation (Figure 9a). Similar findings are observed during negative ENSO situation (Figure 9d). When both the NAO and ENSO are in their negative phases, the anomalous tripole SST pattern is more pronounced (Figure 9g). This suggests that ENSO enhances the connection between the negative NAO and NATI, providing an explanation for the synergistic effects of the NAO and ENSO on dust activities in North China.

In the negative NAO phase, there is a notable correlation between the previous winter NATI and the spring SST and $\mathrm{SST_p}$ (Figures 9b-c), indicating that the previous winter NATI can persist into spring, with the self-persistence of SST playing an important role. Similar findings are observed during the negative ENSO phase (Figures 9e-f) and when both the NAO and ENSO are in their negative phases (Figures 9h-i). Additionally, the correlation coefficients between the NAOI and NATI under different scenarios can illustrate the synergistic influence of the NAO and ENSO on the persistence of SST anomalies (Table 2). Specifically, when the negative phases of NAO and ENSO co-occur, the correlation coefficients between the NAOI and NATI are greater than those influenced by a single factor alone. The impacts of previous winter NAO on the spring dust activities over North China are mainly include, 1) The previous winter NAO would stimulate the anomalous NAT SST pattern; 2) The NAT can persist from previous winter to the following spring due to the thermal persistence of the SST; 3) The spring NAT plays significant modulation on the circulation pattern over North China through teleconnection wave-train, affecting the spring dust activities over North China. It is seen from Table 2 that although the correlation coefficients of previous winter NATI and spring NATI are same in the case of ENSO- phase and NAO- & ENSO- phase. However, the correlations between the NAOI and NATI is higher during NAO- & ENSO- phase (0.66) than during ENSO- phase (0.52), highlighting the a more significant contribution of NAO in influencing NAT in the case of NAO- & ENSO- phase.

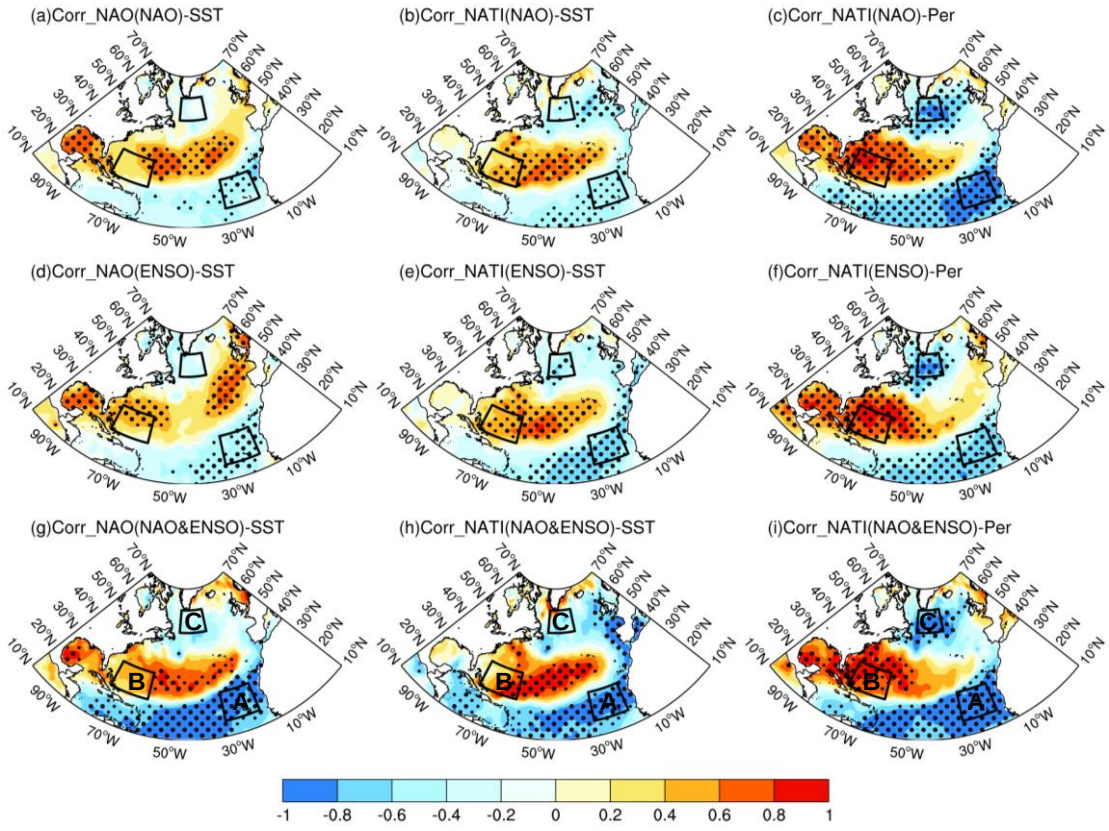

Figure 9. Upper, correlation distributions of (a) winter NAOI with winter SST, (b) winter NATI with spring SST, and (c) winter NATI with SST_p during negative NAO phases. Middle-Lower, as in the upper, but during the negative ENSO phases and concurrent negative phases of NAO and ENSO, respectively. Thick and fine stippled areas are statistically significant at the 0.05 and 0.1 level, respectively. The black box represents NATI.

Table 2. Correlation coefficients between the NAOI and NATI in different categories. * indicates statistically significant at the 0.1 level.

Scenarios	DJF_NAO & DJF _NATI	DJF_NATI & MAM_NATI
NAO^- phase	0.41^*	0.51^*
$ENSO^-$ phase	0.52^*	0.69^*
NAO^- & $ENSO^-$ phase	0.66^*	0.69^*

Given the distance across the Eurasian continent between the North Atlantic and North China, the role of teleconnection wave-train is particularly important in influencing dust activities over North China. Figure 10a presents the geopotential height field at 200 hPa regressed onto the spring NATI during the negative NAO case. This reveals a pronounced north-south reversed dipole pattern in the North Atlantic, i.e., negative over Azores and positive over Iceland, representing a typical negative NAO structure (Wallace and Gutzler, 1981; Li and Wang, 2003). Additionally, a negative-positive-negative teleconnection wave-train structure centered around eastern Europe, Middle East, and North China is observed, suggesting that disturbance energy propagates downstream from the

North Atlantic through waveguide effects. The teleconnection wave-train characteristics are also observed in the 200 hPa meridional wind and vorticity fields (Figures 10b-c). During the negative ENSO case, modulated by the NATI, similar teleconnection structures are also seen in the circulation field (Figures 10d-f). Notably, when both the NAO and ENSO are in their negative phases, the correlation patterns of the teleconnection structure are similar, however the anomalies over North China is enhanced, showing significant anomalies in the vorticity field (Figures 10g-i), confirming their synergistic effects on the circulation processes affecting dust activities in North China.

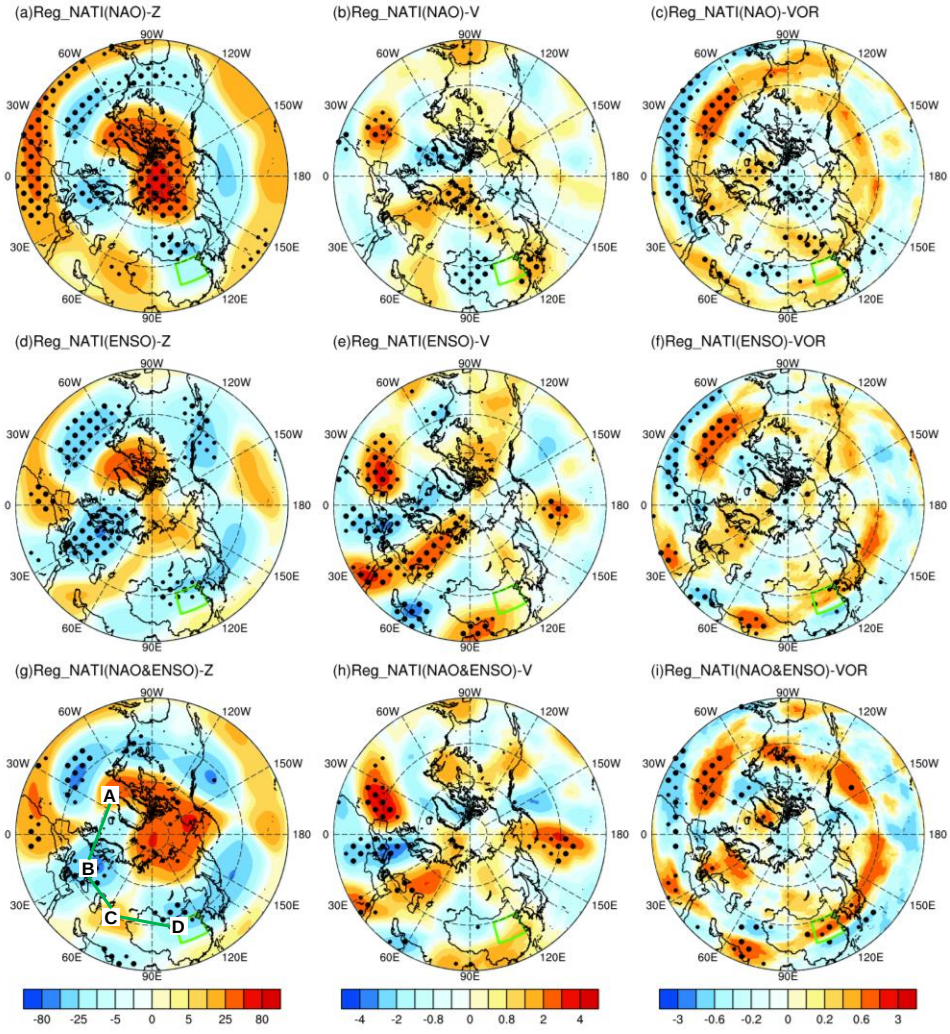

Figure 10. Upper, regression distribution of spring NATI against the spring (a) geopotential height (unit: gpm), (b) meridional wind (unit: $m \cdot s^{-1}$), and (c) vorticity (unit: $10^{-5} \cdot m \cdot s^{-1}$) at 200 hPa during the negative NAO phase. Middle-lower, as in the upper, but during the negative ENSO phases and concurrent negative phases of NAO and ENSO, respectively. The green box represents North China. Regression fields have multiplied by -1 (to facilitate a direct comparison between the NAO&ENSO associated circulation anomalies and the climatology). Thick and fine stippled areas are statistically significant at the 0.05 and 0.1 level, respectively.

To further examine the impact mechanisms of NAO and ENSO on spring dust activities in North China, based on the propagation characteristics of the teleconnection wave-train shown in Figure 10, the cross-section distribution of the geopotential height field is presented (Figure 11). Under the scenarios where either the NAO or ENSO is in the negative phase, the NATI anomalies correspond to the teleconnection wave-train extending from the upper to lower troposphere, which is specifically characterized by a negative-positive-negative teleconnection pattern centered around eastern Europe, Middle East, and North China (Figures 11 a-b). This wave-train propagate across Eurasian continent, ultimately influencing dust activities over North China. Furthermore, the analysis of cross-section at different levels of the troposphere reveals that under the negative NAO and ENSO situations, the teleconnection wave-train excited by the NATI exhibits quasi-barotropic features, with the anomalous structure primarily concentrated in the middle-upper troposphere. When both the NAO and ENSO are in their negative phases, the intensity and scope of the teleconnection wave-train are enhanced and expanded compared to the influence of a single factor (Figure 11c), demonstrating synergistic effects.

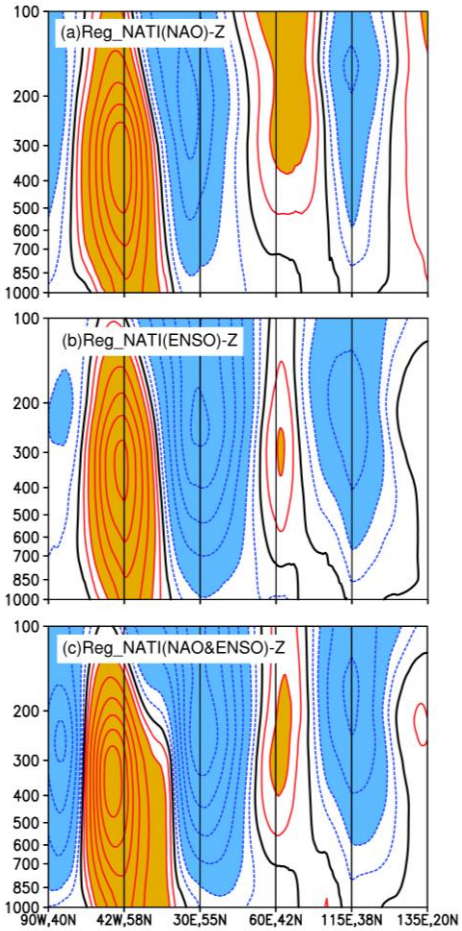

Figure 11. Vertical section of regression of spring NATI against the geopotential height along the solid line labeled A (42°W, 58°N), B (30°E, 55°N), C (60°E, 42°N), and D (115°E, 38°N) in Figure

10g for (a) negative NAO case in the previous winter. (b)-(c) as in (a), but during the negative ENSO case and co-occurring negative phases of NAO and ENSO, respectively (unit: gpm). Regression fields have multiplied by -1 (to facilitate a direct comparison between the NAO&ENSO associated circulation anomalies and the climatology). Shading indicates the absolute value is greater than 10 gpm.

To provide a more comprehensive analysis of the transport process of disturbance energy in the atmosphere, the horizontal distribution of the WAF associated with spring NATI variations is examined. Under the scenarios where either the NAO or ENSO is in the negative phase, the WAF can be clearly observed originating from the North Atlantic, traversing the Eurasian continent, and extending to North China (Figures 12a-b). When both factors occur simultaneously, the transport intensity of the WAF is not only enhanced, but its impact range on dust activities in North China is also broadened (Figure 12c). Through the analysis of teleconnection wave-train and WAF, it is determined that the synergistic effects not only enhance the disturbance intensity in the atmosphere, but also expand impacted extent, thereby promoting the occurrence of spring dust activities in North China. The enhancement and expansion of atmospheric disturbances may be related to large-scale circulation anomalies and local climate condition variations induced by the synergistic effects of the NAO and ENSO, which in turn affect the transport and deposition processes of dust.

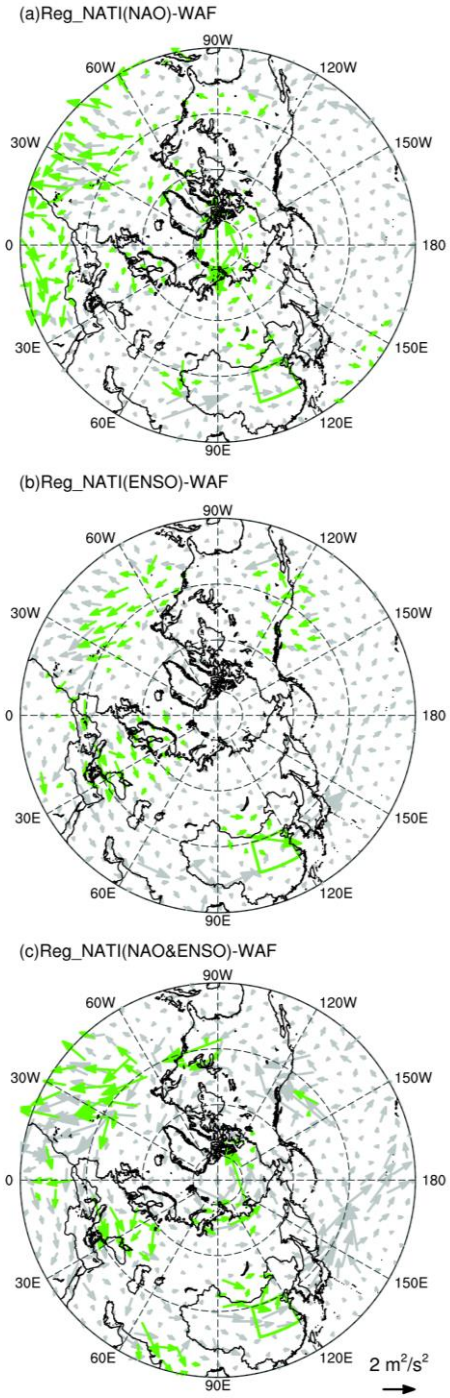

Figure 12. As in Figure 10, but for the regression distribution of spring NATI against the T-N wave activity flux (units: $m^2 \cdot s^{-2}$). The green box represents North China. Regression fields have multiplied by -1 (to facilitate a direct comparison between the NAO&ENSO associated circulation anomalies and the climatology). Green arrows are statistically significant at the 0.1 level.

4. Conclusions and discussions

Although North China is not the primary dust source, dust activities are notably active during

spring in this region. This study highlights that the previous winter NAO and ENSO exert essential influences on the following spring dust activities in North China. Their impacts are asymmetric, manifesting only when both of them are in their negative phases. Furthermore, the results indicate that NAO and ENSO in their negative phases have synergistic effects on the spring dust activities in North China, promoting dust activities and with greater impacts than their sole effect.

Under the influence of the negative phases of the NAO and ENSO, atmospheric circulation in the troposphere from the lower to upper layers, exhibits significant anomalies. These include variations in the upper-level zonal winds, mid-latitude trough-ridge systems, and atmospheric circulation at the SLP. These variations promote the occurrence of dust activities in North China. Simultaneously, accompanying anomalies in the atmospheric circulation pattern also affect local meteorological factors, including humidity and precipitation, which in turn impact dust activities in North China. Notably, when both the NAO and ENSO are in their negative phases, synergistic effects occur, making the anomalies in atmospheric circulation from the lower to upper layers, and local meteorological factors, more conducive to the occurrence of dust events in North China. The impact of the NAO on the underlying SST pattern is predominantly observed during its negative phase, elucidating why the NAO significantly influences dust activities in North China only during its negative phase. Furthermore, when both the NAO and ENSO are in their negative phases, the teleconnection wave-train and WAF stimulated from the North Atlantic are more intense, thereby more effectively influencing dust activities in North China. This indicates the synergistic effects of these two variabilities on dust activities over North China.

In the process where the previous winter NAO influences the following spring dust activities in North China, the NAT plays a crucial role. The NAO signal from the previous winter can be stored in the NAT and persist into spring. In spring, the NAT regulates the circulation pattern in North China through teleconnection wave-train, ultimately affecting dust activities in North China. The signal of previous winter ENSO can persist into spring, and it effects on the dust activities in North China mainly through two pathways: i.e., directly influence the dust activities by affecting the circulation anomalies over the WNP, and facilitating the process of which the NAO excites NAT, thereby affecting the dust activities in North China. This provides a plausible explanation for why the previous winter NAO and ENSO exert synergistic effects on the following spring dust activities in North China.

This study investigated the impacts of NAO and ENSO on dust activities in North China and the associated physical processes, indicating that one season ahead signals provide as the useful predictors for spring dust activities in North China. Future work will focus on developing a

prediction model using the NAO and ENSO as predictors and validating its effectiveness. The present work mainly focuses the interannual modulation of NAO and ENSO on the dust activities over North China, however, the NAO and ENSO (Woollings et al., 2015; Feng et al., 2024), as well as dust activities over North China, bear strong interdecadal variations, long-term datasets are needed to further explore their impacts on the dust activities. The present study focuses on the period 1979-2022, due to the longevity of the MERRA-2 dust content dataset. There are only 7 co-occurrence years of negative NAO and ENSO, which take up to 17% of the whole study period. It is noted that the co-occurrence events are not as many as either the negative NAO or ENSO, thus a significance level of 0.1 is displayed. It is worthy to examine their joint impacts by employing longer datasets or models outputs, to further explore their synergistic effects and any possible variations in their modulations. Moreover, as reported that the state-of-art models can reproduce the individual impact of NAO and ENSO on dust activities in North China (Yang et al., 2022), whether their synergistic effects on the dust activities could be well simulated, requiring further researches. Additionally, the potential impacts of interdecadal signals, such as the AMO, on dust activities in China is not discussed. Future work will investigate the interdecadal variations of dust activities in China and their connection to interdecadal climatic variabilities. Previous studies have indicated that the uncertainty in ENSO variability is likely to increase under the background of global warming (Cai et al., 2021; Chen et al., 2024). Therefore, it is crucial to investigate the future changes in the ENSO and its synergistic effects with NAO on the dust activities over China, to better understand the plausible trends of future dust activities in North China.

Code and data availability. The MERRA-2 dust content dataset can be downloaded from https://disc.gsfc.nasa.gov/datasets?project=MERRA-2 (last access: 22 July 2024). The atmospheric reanalysis datasets can be downloaded from https://cds.climate.copernicus.eu/#!/search?text=ERA5&type=dataset (last access: 22 July 2024). The oceanic reanalysis data can be downloaded from https://www.metoffice.gov.uk/hadobs/hadisst (last access: 22 July 2024). The NAO indices defined by Li and Wang can be downloaded from http://lijianping.cn/dct/page/65610 (last access: 22 July 2024). The NAO indices produce by Hurrell and Jones can be downloaded from https://climatedataguide.ucar.edu/climate-data/hurrell-north-atlantic-oscillation-nao-index-pc-based (last access: 22 July 2024) and https://crudata.uea.ac.uk/cru/data/nao (last access: 22 July 2024), respectively. The ENSO indices can be downloaded from https://psl.noaa.gov/data/timeseries/monthly/NINO34 (last access: 22 July

2024). Our results can be made available upon request.

Author contributions. JF and FLX conceptualized and designed the research. FLX and JF synthesized and analyzed the data. FLX, SW, YL, and JF produced the figures. FLX and SW contributed to the dataset's retrieval. All the authors discussed the results and wrote the paper.

Competing interests. The authors declare that they have no conflict of interest.

Disclaimer. Publisher's note: Copernicus Publications remains neutral with regard to jurisdictional claims in published maps and institutional affiliations.

Acknowledgements. The authors would like to thank the Editor Marco Gaetani and two anonymous reviewers for their useful comments and suggestions that contributed to improving the manuscript. This work was jointly supported by the National Natural Science Foundation of China (42222501) and the BNU-FGS Global Environmental Change Program (No. 2023-GC-ZYTS-03). This work was supported by the National Key Scientific and Technological Infrastructure project "Earth System Numerical Simulation Facility" (EarthLab).

References

Abid, M. A., Kucharski, F., Molteni, F., Kang, I.-S., Tompkins, A. M., and Almazroui, M.: Separating the Indian and Pacific Ocean Impacts on the Euro-Atlantic Response to ENSO and Its Transition from Early to Late Winter, J. Climate, 34, 1531–1548, https://doi.org/10.1175/JCLI-D-20-0075.1, 2021.

Achakulwisut, P., Shen, L., and Mickley, L. J.: What Controls Springtime Fine Dust Variability in the Western United States? Investigating the 2002–2015 Increase in Fine Dust in the U.S. Southwest, J. Geophys. Res.-Atmos., 122, https://doi.org/10.1002/2017JD027208, 2017.

Ayarzagüena, B., Ineson, S., Dunstone, N. J., Baldwin, M. P., and Scaife, A. A.: Intraseasonal Effects of El Niño–Southern Oscillation on North Atlantic Climate, J. Climate, 31, 8861–8873, https://doi.org/10.1175/JCLI-D-18-0097.1, 2018.

Cai, W. J., Santoso, A., Collins, M., Dewitte, B., Karamperidou, C., Kug, J.-S., Lengaigne, M., McPhaden, M. J., Stuecker, M. F., Taschetto, A. S., Timmermann, A., Wu, L. X., Yeh, S.-W., Wang, G. J., Ng, B., Jia, F., Yang, Y., Ying, J., Zheng, X. T., Bayr, T., Brown, J. R., Capotondi, A., Cobb, K. M., Gan, B. L., Geng, T., Ham, Y.-G., Jin, F. F., Jo, H.-S., Li, X. C., Lin, X. P., McGregor, S., Park, J.-H., Stein, K., Yang, K., Zhang, L., and Zhong, W. X.: Changing El Niño–Southern Oscillation in a warming climate, Nat. Rev.-Earth Environ., 2, 628–644, https://doi.org/10.1038/s43017-021-00199-z, 2021.

Chen, S. F., Wu, R. G., and Chen, W.: Strengthened Connection between Springtime North Atlantic Oscillation and North Atlantic Tripole SST Pattern since the Late 1980s, J. Climate, 35, 2007–2022, https://doi.org/10.1175/JCLI-D-19-0628.1, 2020.

Chen, S. F., Chen W., Xie, S. P., Yu, B., Wu, R. G., Wang, Z. B., Lan, X. Q., and Graf. H.: Strengthened impact of boreal winter North Pacific Oscillation on ENSO development in warming climate, npj Climate and Atmospheric Science, 7, 69, https://doi.org/10.1038/s41612-024-00615-3, 2024.

Chen, S. Y., Zhao, D., Huang, J. P., He, J. Q., Chen, Y., Chen, J. Y., Bi, H. R., Lou, G. T., Du, S. K., Zhang, Y., and Yang, F.: Mongolia Contributed More than 42% of the Dust Concentrations in Northern China in March and April 2023, Adv. Atmos. Sci., 40, 1549–1557, https://doi.org/10.1007/s00376-023-3062-1, 2023.

Cressman, G. P.: An operational objective analysis system, Mon. Weather Rev., 87, 367–374, https://doi.org/10.1175/1520-0493(1959)087<0367:AOOAS>2.0.CO;2, 1959.

Csavina, J., Field, J., Félix, O., Corral-Avitia, A. Y., Sáez, A. E., and Betterton, E. A.: Effect of wind speed and relative humidity on atmospheric dust concentrations in semi-arid climates, Sci. Total Environ., 487, 82–90, https://doi.org/10.1016/j.scitotenv.2014.03.138, 2014.

Ding, R. Q., Nnamchi, H. C., Yu, J. Y., Li, T., Sun, C., Li, J. P., Tseng, Y., Li, X. C., Xie, F., Feng, J., Ji, K., and Li, X. M.: North Atlantic oscillation controls multidecadal changes in the North Tropical Atlantic−Pacific connection, Nat. Commun., 14, 862, https://doi.org/10.1038/s41467-023-36564-3, 2023.

Fan, K., Xie, Z. M., Wang, H. J., Xu, Z. Q., and Liu, J. P.: Frequency of spring dust weather in North China linked to sea ice variability in the Barents Sea, Clim. Dyn., 51, 4439–4450, https://doi.org/10.1007/s00382-016-3515-7, 2018.

Feldstein, S. B.: The dynamics of NAO teleconnection pattern growth and decay, Q. J. Roy. Meteor. Soc., 129, 901–924, https://doi.org/10.1256/qj.02.76, 2003.

Feng, J. and Li, J. P.: Influence of El Niño Modoki on spring rainfall over south China, J. Geophys. Res.-Atmos., 116, D13102, https://doi.org/10.1029/2010JD015160, 2011.

Feng, J., Li, J. P., Liao, H., and Zhu, J. L.: Simulated coordinated impacts of the previous autumn North Atlantic Oscillation (NAO) and winter El Niño on winter aerosol concentrations over eastern China, Atmos. Chem. Phys., 19, 10787–10800, https://doi.org/10.5194/acp-19-10787-2019, 2019.

Feng, J., Wang, S., and Li, J. P.: Strengthened ENSO amplitude contributed to regime shift in the Hadley circulation. Geophys. Res. Lett., 51, e2023GL106006. https://doi. org/10.1029/2023GL106006, 2024.

Feng, J., Zhu, J. L., Li, J. P., and Liao, H.: Aerosol concentrations variability over China: two distinct leading modes, Atmos. Chem. Phys., 20, 9883–9893, https://doi.org/10.5194/acp-20-9883-2020, 2020.

Gelaro, R., McCarty, W., Suárez, M. J., Todling, R., Molod, A., Takacs, L., Randles, C. A., Darmenov, A., Bosilovich, M. G., Reichle, R., Wargan, K., Coy, L., Cullather, R., Draper, C., Akella, S., Buchard, V., Conaty, A., Da Silva, A. M., Gu, W., Kim, G.-K., Koster, R., Lucchesi, R., Merkova, D., Nielsen, J. E., Partyka, G., Pawson, S., Putman, W., Rienecker, M., Schubert, S. D., Sienkiewicz, M., and Zhao, B.: The Modern-Era Retrospective Analysis for Research and Applications, Version 2 (MERRA-2), J. Climate, 30, 5419–5454, https://doi.org/10.1175/JCLI-D-16-0758.1, 2017.

Gong, S. L., Zhang, X. Y., Zhao, T. L., Zhang, X. B., Barrie, L. A., McKendry, I. G., and Zhao, C. S.: A Simulated Climatology of Asian Dust Aerosol and Its Trans-Pacific Transport. Part II: Interannual Variability and Climate Connections, J. Climate, 19, 104–122, https://doi.org/10.1175/JCLI3606.1, 2006.

Guo, Y., Li, J. P., and Li, Y.: A Time-Scale Decomposition Approach to Statistically Downscale Summer Rainfall over North China, J. Climate, 25, 572–591, https://doi.org/10.1175/JCLI-D-11-00014.1, 2012.

Hersbach, H., Bell, B., Berrisford, P., Hirahara, S., Horányi, A., Muñoz-Sabater, J., Nicolas, J., Peubey, C., Radu, R., Schepers, D., Simmons, A., Soci, C., Abdalla, S., Abellan, X., Balsamo, G., Bechtold, P., Biavati, G., Bidlot, J., Bonavita, M., De Chiara, G., Dahlgren, P., Dee, D., Diamantakis, M., Dragani, R., Flemming, J., Forbes, R., Fuentes, M., Geer, A., Haimberger, L., Healy, S., Hogan, R. J., Hólm, E., Janisková, M., Keeley, S., Laloyaux, P., Lopez, P., Lupu, C., Radnoti, G., De Rosnay, P., Rozum, I., Vamborg, F., Villaume, S., and Thépaut, J.: The ERA5 global reanalysis, Q. J. Roy. Meteor. Soc., 146, 1999–2049, https://doi.org/10.1002/qj.3803, 2020.

Huang, J., Li, Y., Fu, C., Chen, F., Fu, Q., Dai, A., Shinoda, M., Ma, Z., Guo, W., Li, Z., Zhang, L., Liu, Y., Yu, H., He, Y., Xie, Y., Guan, X., Ji, M., Lin, L., Wang, S., Yan, H., and Wang, G.: Dryland climate change: Recent progress and challenges, Rev. Geophys., 55, 719–778, https://doi.org/10.1002/2016RG000550, 2017.

Huang, J. P., Liu, J. J., Chen, B., and Nasiri, S. L.: Detection of anthropogenic dust using CALIPSO lidar measurements, Atmos. Chem. Phys., 15, 11653–11665, https://doi.org/10.5194/acp-15-11653-2015, 2015.

Huang, Y. H., Liu, X. D., Yin, Z., and An, Z. S.: Global Impact of ENSO on Dust Activities with Emphasis on the Key Region from the Arabian Peninsula to Central Asia, J. Geophys. Res.-Atmos., 126, e2020JD034068, https://doi.org/10.1029/2020JD034068, 2021.

Hurrell, J. W.: Decadal Trends in the North Atlantic Oscillation: Regional Temperatures and Precipitation, Science, 269, 676–679, https://doi.org/10.1126/science.269.5224.676, 1995.

Ji, L. Q. and Fan, K.: Climate prediction of dust weather frequency over northern China based on sea-ice cover and vegetation variability, Clim. Dyn., 53, 687–705, https://doi.org/10.1007/s00382-018-04608-w, 2019.

Jia, X. J., Derome, J., and Lin, H.: Comparison of the Life Cycles of the NAO Using Different Definitions, J. Climate, 20, 5992–6011, https://doi.org/10.1175/2007JCLI1408.1, 2007.

Jiang, W. P., Huang, G., Huang, P., Wu, R. G., Hu, K. M., and Chen, W.: Northwest Pacific Anticyclonic Anomalies during Post–El Niño Summers Determined by the Pace of El Niño Decay, J. Climate, 32, 3487–3503, https://doi.org/10.1175/JCLI-D-18-0793.1, 2019.

Jiménez-Esteve, B. and Domeisen, D. I. V.: The Tropospheric Pathway of the ENSO–North Atlantic Teleconnection, J. Climate, 31, 4563–4584, https://doi.org/10.1175/JCLI-D-17-0716.1, 2018.

Jones, P. D., Jonsson, T., and Wheeler, D.: Extension to the North AtlanticOscillation using early instrumental pressure observations from Gibraltar and South-West Iceland. Int. J. Climatol., 17, 1433–1450, https://doi.org/10.1002/(SICI)1097-0088(19971115)17:13<1433::AID-JOC203>3.0.CO;2-P, 1997.

669 Kang, L. T., Huang, J. P., Chen, S. Y., and Wang, X.: Long-term trends of dust events over Tibetan Plateau during
670 1961-2010, Atmos. Environ., 125, 188-198, https://doi.org/10.1016/j.atmosenv.2015.10.085, 2016.
671 Kim, H. and Choi, M.: Impact of soil moisture on dust outbreaks in East Asia: Using satellite and assimilation data,
672 Geophys. Res. Lett., 42, 2789–2796, https://doi.org/10.1002/2015GL063325, 2015.
673 Kim, S. and Kug, J.: What Controls ENSO Teleconnection to East Asia? Role of Western North Pacific Precipitation
674 in ENSO Teleconnection to East Asia, J. Geophys. Res.-Atmos., 123, https://doi.org/10.1029/2018JD028935,
675 2018.
676 Kok, J. F., Storelvmo, T., Karydis, V. A., Adebiyi, A. A., Mahowald, N. M., Evan, A. T., He, C. L., and Leung, D.
677 M.: Mineral dust aerosol impacts on global climate and climate change, Nat. Rev.-Earth Environ., 4, 71–86,
678 https://doi.org/10.1038/s43017-022-00379-5, 2023.
679 Li, J. P., and Wang, J. X. L.: A new North Atlantic Oscillation index and its variability, Adv. Atmos. Sci., 20, 661–
680 676, https://doi.org/10.1007/BF02915394, 2003.
681 Li, J. P., Zheng, F., Sun, C., Feng, J., and Wang, J.: Pathways of Influence of the Northern Hemisphere Mid-high
682 Latitudes on East Asian Climate: A Review, Adv. Atmos. Sci., 36, 902–921, https://doi.org/10.1007/s00376-
683 019-8236-5, 2019.
684 Li, Y., Xu, F. L., Feng, J., Du, M. Y., Song, W. J., Li, C., and Zhao, W. J.: Influence of the previous North Atlantic
685 Oscillation (NAO) on the spring dust aerosols over North China, Atmos. Chem. Phys., 23, 6021–6042,
686 https://doi.org/10.5194/acp-23-6021-2023, 2023.
687 Liu, X. D., Yin, Z., Zhang, X. Y., and Yang, X. C.: Analyses of the spring dust storm frequency of northern China in
688 relation to antecedent and concurrent wind, precipitation, vegetation, and soil moisture conditions, J. Geophys.
689 Res.-Atmos., 109, 2004JD004615, https://doi.org/10.1029/2004JD004615, 2004.
690 López-Parages, J., Rodríguez-Fonseca, B., and Terray, L.: A mechanism for the multidecadal modulation of ENSO
691 teleconnection with Europe, Clim. Dyn., 45, 867–880, https://doi.org/10.1007/s00382-014-2319-x, 2015.
692 Lou, S. J., Russell, L. M., Yang, Y., Xu, L., Lamjiri, M. A., DeFlorio, M. J., Miller, A. J., Ghan, S. J., Liu, Y., and
693 Singh, B.: Impacts of the East Asian Monsoon on springtime dust concentrations over China, J. Geophys. Res.-
694 Atmos., 121, 8137–8152, https://doi.org/10.1002/2016JD024758, 2016.
695 Lou, S. J., Russell, L. M., Yang, Y., Liu, Y., Singh, B., and Ghan, S. J.: Impacts of interactive dust and its direct
696 radiative forcing on interannual variations of temperature and precipitation in winter over East Asia, J. Geophys.
697 Res.-Atmos., 122, 8761–8780, https://doi.org/10.1002/2017JD027267, 2017.
698 McPhaden, M. J. and Zhang, X. B.: Asymmetry in zonal phase propagation of ENSO sea surface temperature
699 anomalies, Geophys. Res. Lett., 36, 2009GL038774, https://doi.org/10.1029/2009GL038774, 2009.
700 Pan, L. L.: Observed positive feedback between the NAO and the North Atlantic SSTA tripole, Geophys. Res. Lett.,
701 32, 2005GL022427, https://doi.org/10.1029/2005GL022427, 2005.
702 Prospero, J. M., Nees, R. T., and Uematsu, M.: Deposition rate of particulate and dissolved aluminum derived from
703 saharan dust in precipitation at Miami, Florida, J. Geophys. Res.-Atmos., 92, 14723–14731,
704 https://doi.org/10.1029/JD092iD12p14723, 1987.
705 Rayner, N. A., Parker, D. E., Horton, E. B., Folland, C. K., Alexander, L. V., Rowell, D. P., Kent, E. C., and Kaplan,
706 A.: Global analyses of sea surface temperature, sea ice, and night marine air temperature since the late
707 nineteenth century, J. Geophys. Res.-Atmos., 108, 2002JD002670, https://doi.org/10.1029/2002JD002670,
708 2003.
709 Song, L. Y., Chen, S. F., Chen, W., Guo, J. P., Cheng, C. L., and Wang, Y.: Distinct evolutions of haze pollution from
710 winter to following spring over the North China Plain: Role of the North Atlantic sea surface temperature
711 anomalies. Atmos. Chem. Phys., 22, 1669–1688, https://doi.org/10.5194/acp-22-1669-2022, 2022.

Su, J. Z., Zhang, R. H., Li, T., Rong, X. Y., Kug, J., and Hong, C.: Causes of the El Niño and La Niña Amplitude Asymmetry in the Equatorial Eastern Pacific, J. Climate, 23, 605–617, https://doi.org/10.1175/2009JCLI2894.1, 2010.

Sung, M., Lim, G., and Kug, J.: Phase asymmetric downstream development of the North Atlantic Oscillation and its impact on the East Asian winter monsoon, J. Geophys. Res.-Atmos., 115, 2009JD013153, https://doi.org/10.1029/2009JD013153, 2010.

Takaya, K. and Nakamura, H.: A Formulation of a Phase-Independent Wave-Activity Flux for Stationary and Migratory Quasigeostrophic Eddies on a Zonally Varying Basic Flow, J. Atmospheric Sci., 58, 608–627, https://doi.org/10.1175/1520-0469(2001)058<0608:AFOAPI>2.0.CO;2, 2001.

Trenberth, K. E.: The Definition of El Niño, B. Am. Meteorol. Soc., 78, 2771–2777, https://doi.org/10.1175/1520-0477(1997)078<2771:TDOENO>2.0.CO;2, 1997.

Wallace, J. M. and Gutzler, D. S.: Teleconnections in the Geopotential Height Field during the Northern Hemisphere Winter, Mon. Weather Rev., 109, 784–812, https://doi.org/10.1175/1520-0493(1981)109<0784:TITGHF>2.0.CO;2, 1981.

Wang, B., Wu, R. G., and Fu, X. H.: Pacific–East Asian Teleconnection: How Does ENSO Affect East Asian Climate? J. Climate, 13, 1517–1536, https://doi.org/10.1175/1520-0442(2000)013<1517:PEATHD>2.0.CO;2, 2000.

Wang, T. H., Tang, J. Y., Sun, M. X., Liu, X. W., Huang, Y. X., Huang, J. P., Han, Y., Cheng, Y. F., Huang, Z. W., and Li, J. M.: Identifying a transport mechanism of dust aerosols over South Asia to the Tibetan Plateau: A case study, Sci. Total Environ., 758, 11, https://doi.org/10.1016/j.scitotenv.2020.143714, 2021.

Wang, X., Huang, J. P., Ji, M. X., and Higuchi, K.: Variability of East Asia dust events and their long-term trend, Atmos. Environ., 42, https://doi.org/10.1016/j.atmosenv.2007.07.046, 2008

Woollings, T., Franzke, C., Hodson, D. L. R., Dong, B., Barnes, E. A., Raible, C. C., and Pinto, J. G.: Contrasting interannual and multidecadal NAO variability, Clim. Dyn., 45, 539–556, https://doi.org/10.1007/s00382-014-2237-y, 2015.

Wu, J., Kurosaki, Y., Shinoda, M., and Kai, K.: Regional Characteristics of Recent Dust Occurrence and Its Controlling Factors in East Asia, Sola, 12, 187–191, https://doi.org/10.2151/sola.2016-038, 2016.

Wu, R. G. and Chen, S. F.: What Leads to Persisting Surface Air Temperature Anomalies from Winter to Following Spring over Mid- to High-Latitude Eurasia? J. Climate, 33, 5861–5883, https://doi.org/10.1175/JCLI-D-19-0819.1, 2020.

Wu, Z. W., Wang, B., Li, J. P., and Jin, F. F.: An empirical seasonal prediction model of the east Asian summer monsoon using ENSO and NAO, J. Geophys. Res.-Atmos., 114, 2009JD011733, https://doi.org/10.1029/2009JD011733, 2009.

Wu, Z. W., Li, J. P., Jiang, Z. H., He, J. H., and Zhu, X. Y.: Possible effects of the North Atlantic Oscillation on the strengthening relationship between the East Asian Summer monsoon and ENSO, Int. J. Climatol., 32, 794–800, https://doi.org/10.1002/joc.2309, 2012.

Yang, Y., Zeng, L. Y., Wang, H. L., Wang, P. Y., and Liao, H.: Dust pollution in China affected by different spatial and temporal types of El Niño, Atmos. Chem. Phys., 22, 14489–14502, https://doi.org/10.5194/acp-22-14489-2022, 2022.

Yu, Y., Notaro, M., Liu, Z. Y., Wang, F. Y., Alkolibi, F., Fadda, E., and Bakhrjy, F.: Climatic controls on the interannual to decadal variability in Saudi Arabian dust activity: Toward the development of a seasonal dust prediction model, J. Geophys. Res.-Atmos., 120, 1739–1758, https://doi.org/10.1002/2014JD022611, 2015.

Zhang, R. H., Li, T. R., Wen, M., and Liu, L. K.: Role of intraseasonal oscillation in asymmetric impacts of El Niño and La Niña on the rainfall over southern China in boreal winter, Clim. Dyn., 45, 559–567, https://doi.org/10.1007/s00382-014-2207-4, 2015.

Zhang, W. J., Li, J. P., and Jin, F. F.: Spatial and temporal features of ENSO meridional scales, Geophys. Res. Lett., 36, 2009GL038672, https://doi.org/10.1029/2009GL038672, 2009.

Zhang, X. Y., Gong, S. L., Zhao, T. L., Arimoto, R., Wang, Y. Q., and Zhou, Z. J.: Sources of Asian dust and role of climate change versus desertification in Asian dust emission, Geophys. Res. Lett., 30, 2003GL018206, https://doi.org/10.1029/2003GL018206, 2003.

Zhao, C. F., Yang, Y. K., Fan, H., Huang, J. P., Fu, Y. F., Zhang, X. Y., Kang, S. C., Cong, Z. Y., Letu, H., and Menenti, M.: Aerosol characteristics and impacts on weather and climate over the Tibetan Plateau, Natl. Sci. Rev., 7, 492–495, https://doi.org/10.1093/nsr/nwz184, 2020.

Zhao, Y., Huang, A. N., Zhu, X. S., Zhou, Y., and Huang, Y.: The impact of the winter North Atlantic Oscillation on the frequency of spring dust storms over Tarim Basin in northwest China in the past half-century, Environ. Res. Lett., 8, 024026, https://doi.org/10.1088/1748-9326/8/2/024026, 2013.

Zheng, F., Li, J. P., Li, Y. J., Zhao, S., and Deng, D. F.: Influence of the Summer NAO on the Spring-NAO-Based Predictability of the East Asian Summer Monsoon, J. Appl. Meteorol. Clim., 55, 1459–1476, https://doi.org/10.1175/JAMC-D-15-0199.1, 2016a.

Zheng, Y., Zhao, T. L., Che, H. Z., Liu, Y., Han, Y. X., Liu, C., Xiong, J., Liu, J. H., and Zhou, Y. K.: A 20-year simulated climatology of global dust aerosol deposition, Sci. Total Environ., 557–558, 861–868, https://doi.org/10.1016/j.scitotenv.2016.03.086, 2016b.

Zhou, F., Shi, J., Liu, M. H., and Ren, H. C.: Linkage between the NAO and Siberian high events on the intraseasonal timescale, Atmos. Res., 281, 106478, https://doi.org/10.1016/j.atmosres.2022.106478, 2023.

Zhu, C. W., Wang, B., and Qian, W. H.: Why do dust storms decrease in northern China concurrently with the recent global warming? Geophys. Res. Lett., 35, 2008GL034886, https://doi.org/10.1029/2008GL034886, 2008.